Nucleic Acids Research, 2024, **52**, 5209–5225
https://doi.org/10.1093/nar/gkae246
Advance access publication date: 19 April 2024
Molecular Biology

Caspase-mediated processing of TRBP regulates apoptosis during viral infection

Keiko Shibata[1,†], Harune Moriizumi[1,†], Koji Onomoto[2], Yuka Kaneko[1], Takuya Miyakawa[3,4], Shuhei Zenno[5], Masaru Tanokura[3], Mitsutoshi Yoneyama[2,6], Tomoko Takahashi[1,7,*] and Kumiko Ui-Tei[7,8,*]

[1]Department of Biochemistry and Molecular Biology, Graduate School of Science and Engineering, Saitama University, Saitama 338-8570, Japan
[2]Division of Molecular Immunology, Medical Mycology Research Center, Chiba University, Chiba 260-8673, Japan
[3]Department of Applied Biological Chemistry, Graduate School of Agricultural and Life Sciences, The University of Tokyo, Tokyo 113-8657, Japan
[4]Graduate School of Biostudies, Kyoto University, Kyoto 606-8502, Japan
[5]Department of Biotechnology, Faculty of Engineering, Maebashi Institute of Technology, Gunma 371-0816, Japan
[6]Division of Pandemic and Post-disaster Infectious Diseases, Research Institute of Disaster Medicine, Chiba University, Chiba 260-8673, Japan
[7]Department of Biological Sciences, Graduate School of Science, The University of Tokyo, Tokyo 113-0033, Japan
[8]Department of Computational Biology and Medical Sciences, Graduate School of Frontier Sciences, The University of Tokyo, Chiba 277-8561, Japan

[*]To whom correspondence should be addressed. Tel: +81 3 5841 3044; Fax: +81 3 5841 3044; Email: ktei@bs.s.u-tokyo.ac.jp
Correspondence may also be addressed Tomoko Takahashi. Tel: +81 3 5841 3044; Fax: +81 3 5841 3044; Email: takahas@mail.saitama-u.ac.jp
[†]The first two authors should be regarded as Joint First Authors.

Abstract

RNA silencing is a post-transcriptional gene-silencing mechanism mediated by microRNAs (miRNAs). However, the regulatory mechanism of RNA silencing during viral infection is unclear. TAR RNA-binding protein (TRBP) is an enhancer of RNA silencing that induces miRNA maturation by interacting with the ribonuclease Dicer. TRBP interacts with a virus sensor protein, laboratory of genetics and physiology 2 (LGP2), in the early stage of viral infection of human cells. Next, it induces apoptosis by inhibiting the maturation of miRNAs, thereby upregulating the expression of apoptosis regulatory genes. In this study, we show that TRBP undergoes a functional conversion in the late stage of viral infection. Viral infection resulted in the activation of caspases that proteolytically processed TRBP into two fragments. The N-terminal fragment did not interact with Dicer but interacted with type I interferon (IFN) signaling modulators, such as protein kinase R (PKR) and LGP2, and induced ER stress. The end results were irreversible apoptosis and suppression of IFN signaling. Our results demonstrate that the processing of TRBP enhances apoptosis, reducing IFN signaling during viral infection.

Graphical abstract

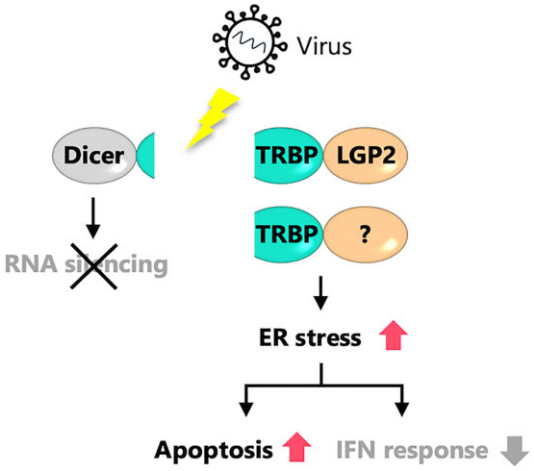

Received: June 29, 2023. **Revised:** March 14, 2024. **Editorial Decision:** March 16, 2024. **Accepted:** March 26, 2024

Introduction

RNA silencing is a post-transcriptional gene-silencing mechanism directed by microRNAs (miRNAs), which are noncoding RNAs approximately 22 nucleotides long. According to release 22 of miRBase, a database of published miRNA sequences, the human genome encodes 1917 miRNA precursors (pre-miRNAs) and 2656 mature miRNAs (1). miRNAs are transcribed from the genome as primary miRNAs (pri-miRNAs) by RNA polymerase II and then processed into pre-miRNAs in the nucleus by a ribonuclease, Drosha (2–6). The pre-miRNAs are exported into the cytoplasm by Exportin-5/Ran-GTP (7,8) and processed into miRNA duplexes by another ribonuclease, Dicer (9). The miRNA duplex is loaded onto Argonaute (AGO); one strand remains on AGO, acting as a primary component of the RNA-induced silencing complex (RISC) (10,11), and the other strand is eliminated (12). In the RISC, miRNAs base-pair with their target mRNAs, and decapping or deadenylation enzymes are recruited to translationally repress the target genes (13–16).

During viral infection, viral RNAs are recognized by virus sensor proteins such as Toll-like receptor 3 (TLR3) (17) and retinoic acid-inducible gene I (RIG-I)-like receptors (RLRs) (18) in the endosome or the cytoplasm. TLR3 and RLRs activate different signaling pathways, but both induce the production of an antiviral cytokine, type I interferon (IFN) (19). Secreted IFN is recognized by IFN-α/β receptor (IFNAR) 1 or IFNAR2 on the cell surface in a paracrine or autocrine manner (20). IFN induces the expression of hundreds of IFN-stimulated genes (ISGs), which function to repress viral replication. TLR3 and RLRs are ISGs, and the positive feedback regulation of these virus sensor proteins by IFN enhances the detection of viral RNA (21,22). The RLRs include RIG-I, melanoma differentiation-associated gene 5 (MDA5), and laboratory of genetics and physiology 2 (LGP2) and are, together with Dicer, members of the RNA helicase family (23–25). RIG-I recognizes RNAs that contain 5′-triphosphate or 5′-diphosphate and small double-stranded RNAs (dsRNAs) as exogenous RNAs (26–32), whereas MDA5 recognizes long dsRNAs (33–36). RIG-I and MDA5 activate the signaling cascade in a manner dependent on their caspase recruitment domains (CARDs), which are necessary for signal transfer to downstream molecules. Among RLRs, LGP2 lacks a CARD, which leaves its function unclear.

TRBP is an RNA-silencing enhancer with three dsRNA-binding domains (dsRBDs): dsRBD1, dsRBD2 and dsRBD3. dsRBD1 and dsRBD2 bind to pre-miRNAs, whereas dsRBD3 interacts with Dicer (37–41). In human cells, TRBP prefers to bind pre-miRNAs that have tight base pairing in the stem, thereby enhancing the recruitment of pre-miRNAs to Dicer (24). TRBP-bound miRNAs target apoptosis-regulatory genes, including initiator and executioner caspases (caspase-2, 3, 7 and 8) (42). TRBP interacts with LGP2, which represses RNA silencing directed by TRBP-bound miRNAs to upregulate apoptosis-regulatory genes and so enhance apoptosis in the early stage of viral infection (24,42). RNA silencing is mediated by endogenous miRNAs, and IFN signaling is triggered by exogenous viral RNAs, which were formerly considered independent pathways. However, these engage in crosstalk, and TRBP functions as a reversible hub molecule between RNA silencing and IFN signaling. Here we show functional conversion of TRBP in the late stage of viral infection. TRBP is irreversibly processed by active caspase(s) and proteolytically processed into N- and C-terminal fragments (TRBP-N and TRBP-C). The processing of TRBP enhances apoptosis during viral infection, thereby suppressing IFN signaling. Our findings suggest that TRBP undergoes a functional conversion by means of processing by caspase(s) during viral infection of mammalian cells. This study provides a significant insight which clearly revealed that RNA silencing mechanism, which is known to be an antiviral mechanism in plant or invertebrate, is strongly related to antiviral response also in mammals, although the mechanism is completely different.

Materials and methods

Cell culture

Human HeLa wild-type (WT) or TRBP$^{-/-}$ cells generated by CRISPR genome editing (24) were cultured in Dulbecco's modified Eagle's medium (Wako) containing 10% fetal bovine serum (NICHIREI) and antibiotics [100 U/ml of penicillin and 100 μg/mol of streptomycin (Sigma-Aldrich)] at 37°C with 5% CO_2.

Plasmid construction

The expression plasmids of TRBP or PACT (pcDNA5-FLAG-TRBP, pET28a-TRBP, pET28a-PACT) were constructed as described previously (24,41). Plasmid encoding TRBP without epitope tag (pcDNA3-TRBP2) was kindly provided by Dr A. Gatignol (43,44). The site-directed mutagenesis was carried out to generate the expression constructs of TRBP-D234A, D254A, or D266A using pET28a-TRBP and pcDNA3-TRBP2, whose aspartic acid residue at 234, 255 or 266 was replaced with alanine (pET28a-TRBP-D234A, D254A or D266A, and pcDNA3-TRBP2-D234A, D254A or D266A). Plasmid expressing the N-terminal or C-terminal fragment of TRBP (pcDNA5-FLAG-TRBP-N, or C) was generated by amplification of each fragment by PCR and ligation using the KOD-Plus-Mutagenesis Kit (TOYOBO) and DNA Ligation Kit (TAKARA Bio). The expression plasmid of pre-miRNA-like RNA targeting firefly luciferase, pre-miLuc (pSilencer-FL774) was constructed as described previously (45). The plasmids were purified using the Genopure Plasmid Midi Kit (Roche). The oligonucleotide sequences used for plasmid construction were shown in Supplementary Table S1.

Viral infection

Newcastle disease virus (NDV, Miyadera strain), Sendai virus (SeV, Cantell Strain), or Influenza A virus (IAV, PR8 strain) was incubated with serum-free medium for 1 h at 37°C. After adsorption, the medium was changed into a serum-containing medium and cultured at 37°C with 5% CO_2. The Multiplicity of Infection (MOI) for SeV infection determined by plaque assay was 15.

Polyinosinic:polycytidylic acid [poly(I:C)] transfection and tumor necrosis factor α (TNFα)/cycloheximide (CHX) treatment

A cell suspension (2×10^5 cells/well) was plated into a 12-well plate 1 day before plasmid transfection with polyinosinic:polycytidylic acid [poly(I:C)] (2 μg/ml) or the treatment of tumor necrosis factor α (TNFα) (10 ng/ml) and cycloheximide (CHX) (20 μg/ml). The cells were collected at

0, 6 and 9 h following poly(I:C) transfection or TNFα/CHX treatment.

Western blot

The samples were mixed with 2× sodium dodecyl sulfate-polyacrylamide gel electrophoresis (SDS-PAGE) sample buffer and heated at 95°C for 5 min. The samples were separated by SDS-PAGE and transferred to a polyvinylidene fluoride (PVDF) membrane using the Trans-Blot Turbo Transfer System (Bio-Rad). The membrane was blocked for 1 h in Tris-buffered saline-Triton X-100 or Tween 20 (TBS-T) supplemented with 5% skim milk and incubated with specific antibodies in Can Get Signal immunoreaction enhancer solution (TOYOBO) at 4°C overnight. Antibodies against TRBP (AbFrontier), AGO2 (Wako), PACT (Santa Cruz Biotechnology), PKR (Santa Cruz Biotechnology), pro-caspase-3 (abcam), active caspase-3 (abcam), β-actin (MBL), and FLAG (Cell Signaling) were used. Antibodies against Dicer, RIG-I, MDA5 and LGP2 were generated by immunizing rabbits with synthetic peptides (9,46). The membrane was washed three times with TBS-T and reacted with HRP-linked anti-rabbit or -mouse antibody (GE Healthcare) at room temperature for 1 h. The membrane was washed three times with TBS-T and reacted with ECL Prime Western Blotting Detection Reagent (GE Healthcare). The visualization was performed using the ImageQuant LAS4000 Mini imager (GE Healthcare).

The purification of recombinant TRBP or PACT protein

The purification of recombinant TRBP or PACT protein was described previously (41). Briefly, the expression plasmid of TRBP or PACT was transformed into *Escherichia coli* Rosetta (DE3) pLysS and cultured to an OD_{600} of 0.6 in Luria-Bertani (LB) medium. After culturing for 6 h with 0.3 mM isopropyl β-D-thiogalactoside (IPTG), cells were collected and lysed by sonication. The purification was performed with Ni-NTA agarose (QIAGEN) according to the manufacturer's protocol. The eluted samples were exchanged to the buffer containing 20 mM Tris–HCl (pH8.0), 300 mM NaCl and 10% glycerol using PD-10 desalting columns (GE healthcare). The purities were confirmed by performing SDS-PAGE and subsequent Coomassie Brilliant Blue (CBB) staining. The protein concentration was determined by Protein Assay (Bio-Rad).

In vitro caspase-3 assay

The recombinant TRBP or PACT protein was incubated with active caspase-3 protein (1 unit/μL) (Abcam) in *in vitro* caspase assay buffer containing 50 mM Tris–HCl (pH7.5), 50 mM NaCl, 10 mM EDTA, 10 mM dithiothreitol and 5% glycerol, at 37°C. The reaction was stopped by adding 2× SDS-PAGE sample buffer and boiling for 5 min. The samples were separated by SDS-PAGE on 12.5% denatured polyacrylamide gel and stained with CBB.

N-terminal amino acid sequencing

The recombinant TRBP proteins were incubated with active caspase-3 proteins (Abcam) for 4 h at 37°C. The samples were separated by SDS-PAGE on 12.5% denatured polyacrylamide gel and transferred to the PVDF membrane. The membrane was stained with CBB. The C-terminal fragment of processed TRBP was excised from the membrane and purified to be analyzed by N-terminal amino acid sequencing.

Inhibition of caspase activity using siRNAs or inhibitors

A cell suspension (2×10^5 cells/well) of HeLa cells was plated into a 12-well plate 1 day before transfection, and siRNA against caspase-2, 3, 7 or 8 was transfected into the cells. Viral infection was performed 1 day following the transfection, and the cells were lysed for Western blots. For the experiments using caspase inhibitors, caspase-1 inhibitor (Ac-YVKD-CHO; Peptide institute, Inc.) or caspase-3 inhibitor (Ac-DMQD-CHO; Peptide institute, Inc.) was added to the cells before viral infection.

Electrophoresis mobility shift assay

The electrophoresis mobility shift assay of recombinant TRBP protein was described previously (41). Briefly, the recombinant TRBP protein was incubated with ^{32}P-labeled miLuc-1 or miLuc-2 for 30 min on ice in EMSA binding buffer containing 20 mM Tris–HCl [pH8.0], 1.5 mM $MgCl_2$, 50 mM NaCl, 1.5 mM DTT, 100 ng/μl sonicated salmon sperm DNA, 5% glycerol and 0.4 U/ml RNasein (Promega). The samples were electrophoresed on a 9% non-denatured polyacrylamide gel in 0.25× TBE buffer. The visualization was performed using the Fuji imaging plate and Typhoon image analyzer (GE Healthcare).

Immunoprecipitation

A HeLa cell suspension (7×10^5 cells/well) was plated into a 6-well plate 1 day before plasmid transfection with human type-I IFN (IFNα1; Cell Signaling). Cells were washed with phosphate-buffered saline and lysed in cold lysis buffer (10 mM Hepes–NaOH [pH 7.9], 1.5 mM $MgCl_2$, 10 mM KCl, 0.5 mM DTT, 140 mM NaCl, 1 mM EDTA, 1 mM Na_3VO_4, 10 mM NaF, 0.5% NP-40, and complete protease inhibitor) 24 h following the plasmid transfection, then the cell lysates were centrifuged at 14 000 rpm for 10 min. For immunoprecipitation, 30 μl of Dynabeads Protein G (Thermo Fisher Scientific) was mixed with 2.5 μg of mouse anti-FLAG antibody (Sigma), or 2.5 μg of mouse IgG (Santa Cruz Biotechnology) as a negative control and rotated at 4°C for 2 h. The cell lysates in the presence or absence of RNase V1 (0.3 U/ml; Ambion) were then mixed with the antibody-bound Dynabeads Protein G and rotated at 4°C for 2 h. The beads were washed twice with wash buffer containing 300 mM NaCl and once with lysis buffer. To elute the bound proteins, 2× SDS-PAGE sample buffer (30 μl) was added, and the beads were heated at 95°C for 5 min.

RNA silencing activity assay

RNA silencing activity was measured with a dual luciferase reporter assay. A $TRBP^{-/-}$ cell suspension (1.0×10^5 cells/ml) was inoculated in a 24-well plate 1 day before transfection. Cells were transfected with 0.5 μg of pGL3-Control vector (Promega) encoding the firefly *luciferase* gene, 0.1 μg of pRL-SV40 vector (Promega) encoding the *Renilla luciferase* gene, 5 ng of pSilencer-3.1-H1-puro vector encoding pre-miLuc (pSilencer-FL774) against the firefly *luciferase* with Lipofectamine 2000 reagent (Invitrogen). Viral infection was performed 1 day following the transfection, and the cells were

lysed with 1× passive lysis buffer (Promega). Luciferase activity was measured using the Dual-Luciferase Reporter Assay System (Promega), and the firefly luciferase activity normalized to that of *Renilla* luciferase (firefly luciferase activity / *Renilla* luciferase activity) was determined.

Detection of apoptotic cells using Annexin V

TRBP$^{-/-}$ cells in a well of 12-well plate (3.0×10^5 cells/ml/well) were transfected with plasmid encoding TRBP-WT or -D234A 1 day before viral infection. Apoptotic cell death was determined by Annexin V-FITC Apoptosis Detection Kit (nacalai tesque) and fluorescence microscope at 24 h following SeV infection according to the manufacturer's instruction.

Microarray analysis

Human HeLa TRBP$^{-/-}$ cells transfected with plasmid encoding TRBP-WT, -N or -D234A were collected at 24 h following SeV infection. Total RNA was extracted using the FastGene RNA Premium Kit (Nippon Genetics). The quality of the total RNA was confirmed using the Bioanalyzer (Agilent Technologies), and cDNA and Cy-3-labeled RNA were synthesized using the Quick Amp Labeling kit for One Color (Agilent Technologies). Cy-3-labeled RNA was fragmented using the Gene Expression Hybridization Kit (Agilent Technologies) and hybridized to SurePrint G3 Human GE Microarray version 3 (Agilent Technologies) at 65°C for 17 h. After being washed, the microarray slide was scanned by DNA Microarray Scanner (Agilent Technologies) and the signals were quantified by Feature Extraction software (Agilent Technologies). Data analysis was performed on probes that passed filtering, and gene ontology (GO) analysis was performed by the DAVID online software tool (47).

Small RNA sequencing (RNA-seq) analysis

Human HeLa wild-type (WT) or TRBP$^{-/-}$ cells were plated into a well of 12-well plate (3.0×10^5 cells/ml/well) 1 day before viral infection, and SeV was infected. The cells were collected at 18 h following SeV infection. Total RNA was extracted by ISOGEN II (Nippongene) according to the manufacturer's instruction and the qualities were confirmed by Bioanalyzer (Agilent Technologies). Unique Molecular Identifier (UMI) small RNA libraries were generated and small RNA-seq was carried out using Digital NanoBiotechnology sequencing (DNBseq) in single-end mode by Beijing Genomics Institute (BGI). All of the 36 nt reads were mapped to the RefSeq sequences (GRCh38.p14) using STAR sequence aligner according to the miRNA database (miRBase release 22). After counting raw reads using featureCounts, reads corresponding to mature miRNAs were normalized by Transcripts Per Million (TPM). SeV/mock was calculated by the following formula: $(SeV_{TPM} + 1)/(mock_{TPM} + 1)$.

Quantitative reverse transcription (qRT)-PCR

Total RNA was extracted using the FastGene RNA Premium Kit (Nippon Genetics). The total RNA (0.2 μg) was used for cDNA synthesis with the High-Capacity cDNA Reverse Transcription Kit (Applied Biosystems). qRT-PCR was performed using the KAPA SYBR Fast qPCR Master Mix (Kapa Biosystems) with the StepOnePlus Real-Time PCR System or QuantStudio 3 Real-Time PCR System (Applied Biosystems). For the detection of mature miRNAs, total RNA including small RNAs was extracted using the FastGene RNA Premium Kit with FastGene miRNA enhancer. The extracted RNA (0.2 μg) was used for cDNA synthesis using specific stem-loop RT primers. The primer sequences were shown in Supplementary Table S2.

Alignment of the amino acid sequence of TRBP

The amino acid sequences of TRBP were obtained from RefSeq: *Homo sapiens* (NP_599150), *Mus musculus* (NP_033345.2), *Rattus norvegicus* (NP_001030113.1), *Oryctolagus cuniculus* (XP_002711070.1), *Callithrix jacchus* (XP_002752581.1), *Bos taurus* (NP_001069146.2), *Equus caballus* (XP_001504584.1), *Sus scrofa* (XP_003126242.1), *Ailuropoda melanoleuca*, XP_002923310.1), *Pongo abelii* (XP_002823375.2), *Gorilla gorilla gorilla* (XP_004053284.1), *Drosophila melanogaster* (NP_609646.1), *Caenorhabditis elegans* (NP_499265.1), *Danio rerio* (NP_956291.1), *Xenopus laevis* (NP_001085574.1), *Columba livia* (XP_005514793.1), *Anolis carolinensis* (XP_003216784.1) and *Penaeus monodon* (AGD81191.1). The amino acid sequences of TRBP were analyzed by the ClustalW (48).

Results

TRBP is processed during viral infection

Multiple dsRNA-binding proteins are involved in the regulation of miRNA-mediated RNA silencing. However, the regulatory mechanism of the antiviral function of RNA silencing is unclear. To investigate protein levels of regulators during viral infection, we infected Newcastle disease virus (NDV), Sendai virus (SeV), or influenza A virus (IAV) into human HeLa cells, and harvested them 0, 6, 10, 14, 18 and 24 h after infection. These viruses are negative-sense single-stranded RNA viruses that are recognized by an RLR-family protein, RIG-I. The mRNA level of IFN-β is upregulated in cells infected with NDV or SeV but not in cells infected with IAV (42). Western blotting showed that protein levels of RIG-I, MDA5 and LGP2 were upregulated, likely in a manner involving secreted IFN, in SeV-infected cells (Figure 1A). However, these IFN-induced proteins were not upregulated during NDV infection, because NDV induced the phosphorylation of dsRNA-dependent protein kinase (PKR) and blocked *de novo* protein synthesis (Figure 1A). The expression patterns of RLRs during viral infection were consistent with previous reports (42). Here, we evaluated protein levels of regulators of RNA silencing (AGO2, Dicer and TRBP) using Western blotting during viral infection (Figure 1A). The band patterns of Dicer and AGO2 showed no significant changes in cells infected with NDV, SeV, and IAV. By contrast, those of TRBP changed over time following NDV or SeV infection. The signal intensity of full-length TRBP decreased, and the signal intensity of low-molecular-weight TRBP increased, ≥18 h after NDV or SeV infection. IAV infection had little effect on the protein level of TRBP. TRBP enhances the maturation of TRBP-bound pre-miRNAs by interacting with Dicer (42). However, the TRBP–Dicer interaction is suppressed by the enhanced interaction of TRBP with LGP2 during viral infection. As a result, the expression of target genes repressed by miRNAs maturated from TRBP-

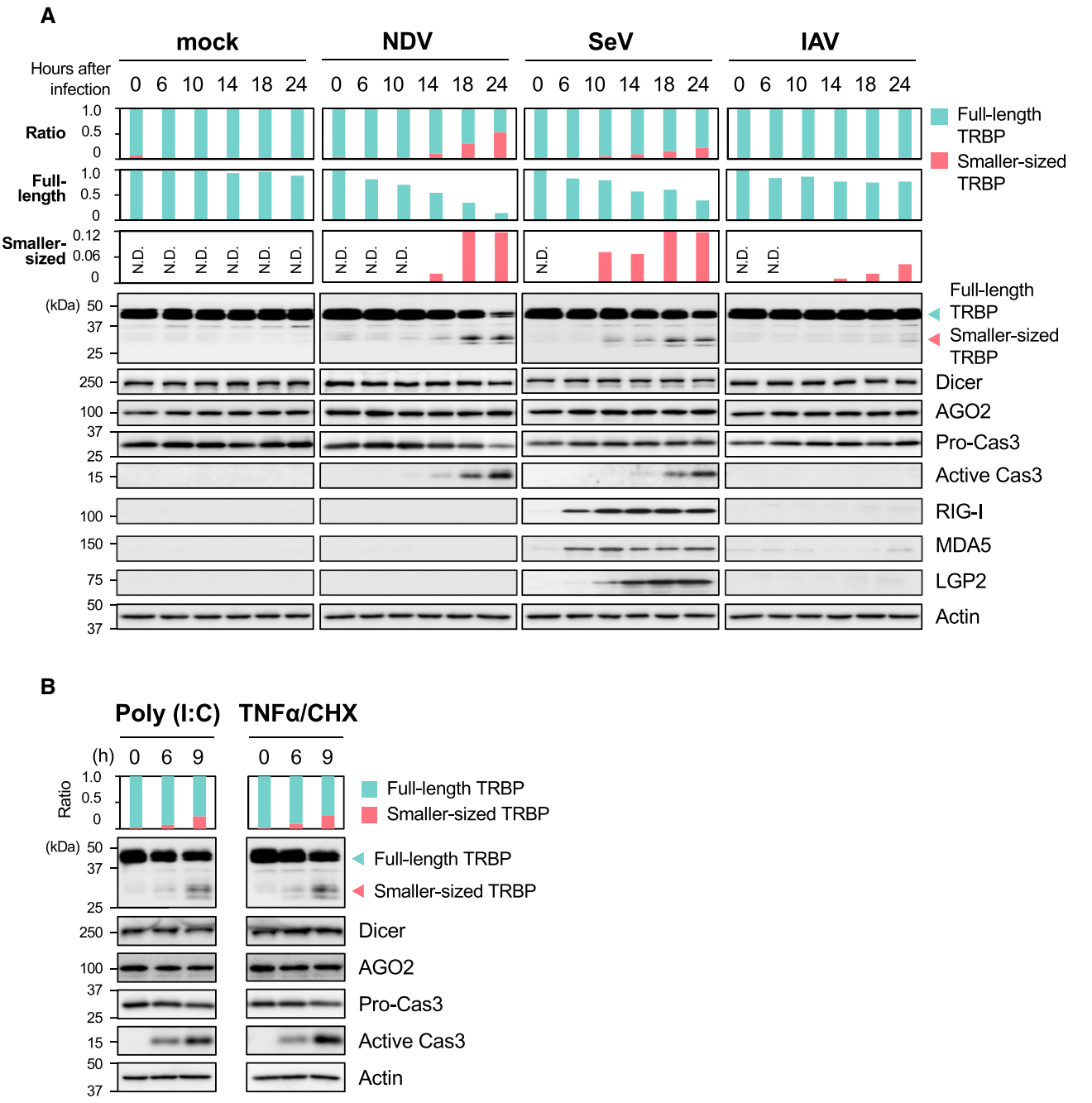

Figure 1. An enhancer of RNA silencing, TRBP, is processed during viral infection. (**A**) Western blotting of endogenous TRBP, Dicer, AGO2, pro-caspase-3, active caspase-3, RIG-I, MDA5, LGP2, and actin in mock-treated or virus (NDV, SeV or IAV)-infected cells. (**B**) Western blotting of TRBP, Dicer, AGO2, pro-caspase-3, active caspase-3, and actin in poly(I:C)-transfected or TNFα/CHX-treated cells. Band intensities were quantified, and the ratio of full-length TRBP (green) to smaller TRBP (pink) was determined.

bound pre-miRNAs via the TRBP–Dicer interaction was upregulated. The upregulated genes include caspases-2, 3, 7 and 8, which are regulators of apoptosis (42). Therefore, the upregulated caspases may process TRBP during viral infection. Western blotting showed that caspase-3 was activated ≥ 18 h after NDV or SeV infection (Figure 1A). Transfection of poly(I:C) (2 μg/ml), treatment with TNFα and CHX (Figure 1B), and infection by NDV or SeV increased protein levels of low-molecular-weight TRBP and activated caspase-3. These results suggested that TRBP, but not Dicer or AGO2, was processed by caspase-like activities during NDV or SeV infection.

TRBP is processed by caspase-3

To examine whether TRBP is processed by caspase-3, we purified recombinant TRBP proteins and incubated them with active caspase-3 *in vitro* (Figure 2A). The purification procedure was described previously (41). The purified recombinant TRBP proteins were incubated with or without active caspase-3 at 37°C for 1 h. The samples were electrophoresed on 12.5% denatured polyacrylamide gels and stained with CBB. Full-length TRBP (45 kDa) was processed into two low-molecular-weight fragments (29 and 16 kDa, respectively).

The human genome encodes multiple caspases, which have overlapping consensus motifs for target recognition and

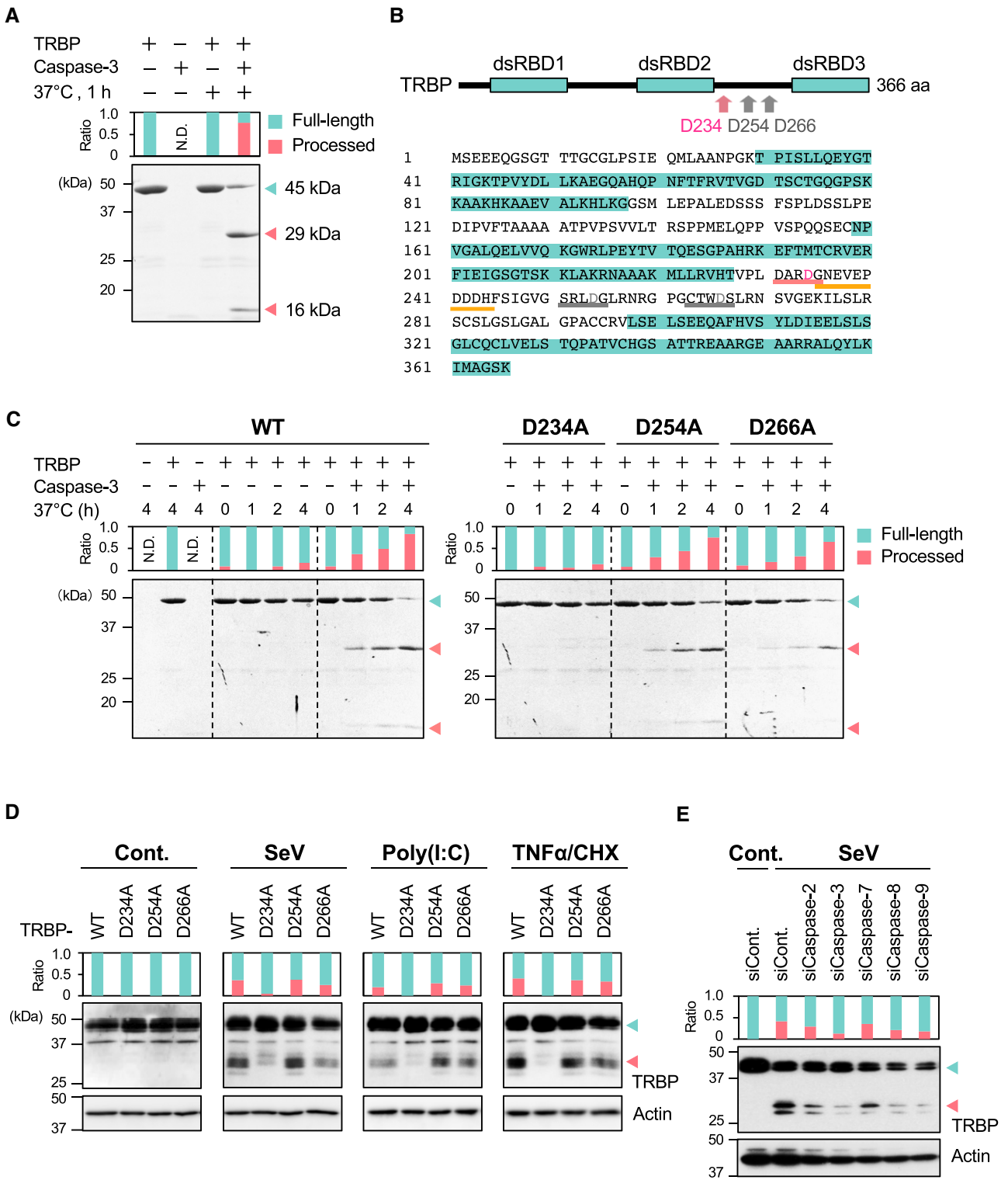

Figure 2. TRBP is processed by caspase-3. (**A**) *In vitro* caspase-3 assay using recombinant TRBP-WT proteins. TRBP proteins were incubated with active caspase-3 and electrophoresed in a 12.5% acrylamide denaturing gel, followed by CBB staining. Band intensities were quantified, and the ratio of full-length TRBP (45 kDa, green) to processed TRBP (29 + 16 kDa, pink) was determined. (**B**) Domain structure and amino acid sequence of TRBP. The orange underlining shows the processed TRBP (16 kDa) region subjected to N-terminal amino acid sequencing. (**C**) *In vitro* caspase-3 assay using TRBP-WT, D234A, D254A or D266A. (**D**) Western blotting of endogenous TRBP and actin in mock-treated, SeV-infected, poly(I:C)-transfected, or TNFα/CHX-treated TRBP$^{-/-}$cells. Cells were transfected with a plasmid encoding TRBP-WT, D234A, D254A, or D266A without an epitope tag. The amounts of transfected plasmids were consistent with the levels of endogenous TRBP proteins in WT cells. (**E**) Western blotting of endogenous TRBP and actin in WT cells transfected with an siRNA against caspase-2, 3, 7, 8 or 9.

cleavage. The favored motif of active caspase-3 is DxxD/G (49–51), which is consistent with the amino acid sequence at positions D231 to G235 of TRBP (DARD/G) (Figure 2B, pink underline). To determine whether TRBP is processed by caspase-3 between D234 and G235, we generated a recombinant mutant TRBP, TRBP-D234A, in which the aspartic acid residue at position 234 was substituted for alanine and purified as for wild-type TRBP (TRBP-WT; Supplementary Figure S1). We performed an *in vitro* caspase-3 assay; TRBP-WT, but not TRBP-D234A, was processed by active caspase-3 (Figure 2C). The favored motif of active caspase-3 was conserved at D254 (SRLD/G) but not D266 (CTWD/S) (Figure 2B, gray underline). We generated other TRBP mutants in which the aspartic acid at position 254 or 266 was substituted for alanine (TRBP-D254A and -D266A). TRBP-D254A and -D266A were processed by caspase-3; therefore, TRBP was processed by active caspase-3 at D234/G235, but not D254/G255 or D266/S267, *in vitro*. The band of low-molecular-weight of TRBP (16 kDa) was excised from the PVDF membrane and subjected to N-terminal amino acid sequencing. The N-terminal amino acid sequence was Gly Asn-Glu-Val-Glu-Pro-Asp-Asp-Asp-His (GNEVEPDDDH; Supplementary Figure S2), consistent with that of G235 to H244 of full-length TRBP (Figure 2B, orange underline). Therefore, TRBP was processed into two fragments between D234 and G235 by caspase-3 *in vitro*.

To determine whether TRBP is processed between D234 and G235 in human cells, we transfected the plasmid encoding TRBP-WT, -D234A, -D254A or -D266A lacking an epitope tag into TRBP$^{-/-}$ cells, which were generated by CRISPR/Cas genome engineering (24). The concentration of transfected plasmid (0.01 μg/well) was consistent with the level of endogenous TRBP protein in WT cells (Supplementary Figure S3). One day after transfection, SeV infection, poly(I:C) transfection, or TNFα/CHX treatment was performed and TRBP proteins were detected by Western blotting using an anti-TRBP antibody (Figure 2D). Low-molecular-weight TRBP was detected in TRBP-WT-, -D254A- and -D266A-transfected cells, but not in TRBP-D234A-transfected cells, which indicates that TRBP is processed between D234 and G235 in human cells *in vivo* as well as *in vitro*.

Caspases-2, -8 and -9 are initiator caspases, and caspases-3 and -7 are executioner caspases (52,53). Extrinsic death signals activate caspase-8, and intrinsic stress signals activate caspase-9. Caspase-2 is believed to induce apoptosis via both extrinsic and intrinsic pathways (53). To investigate the involvement of other caspases in the processing of TRBP, we transfected cells with an siRNA against each of caspases-2, -3, -7, -8 and -9 prior to viral infection (Figure 2E and Supplementary Table S3). mRNA levels of caspases-2, -3, -7, -8 and -9 decreased by 34.4%, 33.2%, 37.0%, 31.4% and 29.8% after siRNA transfection, respectively (Supplementary Figure S4). The knockdown of caspases-3, -8 and -9 decreased the level of processed TRBP. Serial or parallel regulation of caspase-3 by caspases-8 and -9 via the extrinsic and intrinsic apoptosis pathways has been reported (54). The treatment of caspase-3 inhibitor (Ac-DMQD-CHO) also repressed the processing of TRBP, but that of caspase-1 inhibitor (Ac-YVKD-CHO) did not (Supplementary Figure S5). These findings suggest that caspase-3 is involved in the processing of TRBP.

A protein activator of PKR (PACT) consists of three dsRBDs and modulates RNA silencing by interacting with Dicer, although its precise function is unclear. To determine whether PACT is processed by caspase-3, we purified recombinant PACT proteins and subjected them to *in vitro* caspase-3 assay. PACT was not processed by caspase-3 (Supplementary Figure S6), consistent with its lack of the favored motif of caspases. Therefore, TRBP, but not PACT, was processed by caspase(s) during viral infection of human cells.

Processed TRBP interacts with IFN modulators but not with RNA-silencing factors

TRBP binds to pre-miRNA via dsRBD1 and dsRBD2 and interacts with Dicer via dsRBD3 to enhance miRNA maturation (Figure 3A and B) (39–41). To examine the dsRNA-binding affinity of processed TRBP, we purified the recombinant N- and C-terminal fragments (TRBP-N or -C) in addition to TRBP-WT (Supplementary Figure S7A). We performed electrophoresis mobility shift assay (EMSA) of TRBP proteins using dsRNAs with a 2 nt 3′-overhang resembling a miRNA duplex that targets firefly luciferase, miLuc-1 (Figure 3C and D). ^{32}P-labeled miLuc-1 was incubated with TRBP proteins and separated on non-denatured polyacrylamide gels. At low concentrations of TRBP, TRBP-WT bound to miLuc-1 as a monomer (complex 1), and at high concentrations it bound as a dimer (complex 2) (41). These results show that TRBP-N, but not TRBP-C, binds to miLuc-1 similarly to TRBP-WT (Figure 3D and E). Comparable results were obtained for another miRNA duplex, miLuc-2 (Supplementary Figure S7), which indicates that TRBP-N has dsRNA-binding activity.

LGP2 is upregulated by IFN and interacts with TRBP via dsRBD1 and dsRBD2 to inhibit pre-miRNA binding to TRBP (24). Furthermore, the interaction of TRBP with LGP2 inhibits the interaction of TRBP with Dicer (42). To examine the interactions of processed TRBP, we transfected a plasmid encoding each FLAG-tagged TRBP protein (TRBP-WT, -N and -C) into IFN-treated TRBP$^{-/-}$ cells and performed immunoprecipitation using an anti-FLAG antibody (Figure 3F). The IFN treatment alone does not induce the activation of caspase-3 and the processing of TRBP (Supplementary Figure S8). The presence of TRBP-WT or -N was confirmed in the input sample and either protein immunoprecipitated with the anti-FLAG antibody; TRBP-C was absent from the input sample but was present at a low level in the immunoprecipitated sample, as determined by Western blotting (Figure 3F, long exposure). Reverse transcription PCR (RT-PCR) using purified total RNAs detected TRBP-C, -WT and -N mRNAs, which suggests that the C-terminal portion of TRBP is unstable (Supplementary Figure S9). Dicer or PACT interacted with TRBP and immunoprecipitated with TRBP-WT. However, the interaction of TNBP-N with Dicer was almost completely abolished and the interaction with PACT was suppressed. The IFN-signaling modulators PKR and LGP2 immunoprecipitated with TRBP-N and -WT. These results indicate that TRBP converted preferable protein partners from RNA-silencing regulators to IFN-signaling modulators. Immunoprecipitation with RNase V1, a non-sequence-specific dsRNA nuclease, showed no significant difference, indicating that these interactions are RNA-independent (Supplementary Figure 10). TRBP enhances the maturation of miRNAs by interacting with pre-miRNAs and Dicer (39–41). After processing, the N-terminal portion of TRBP did not show decreased dsRNA-binding activity; by contrast, the interaction of TRBP with LGP2 inhibits the binding of TRBP to pre-miRNAs (24). Furthermore, processed TRBP lost its ability to interact with Dicer but exhibited

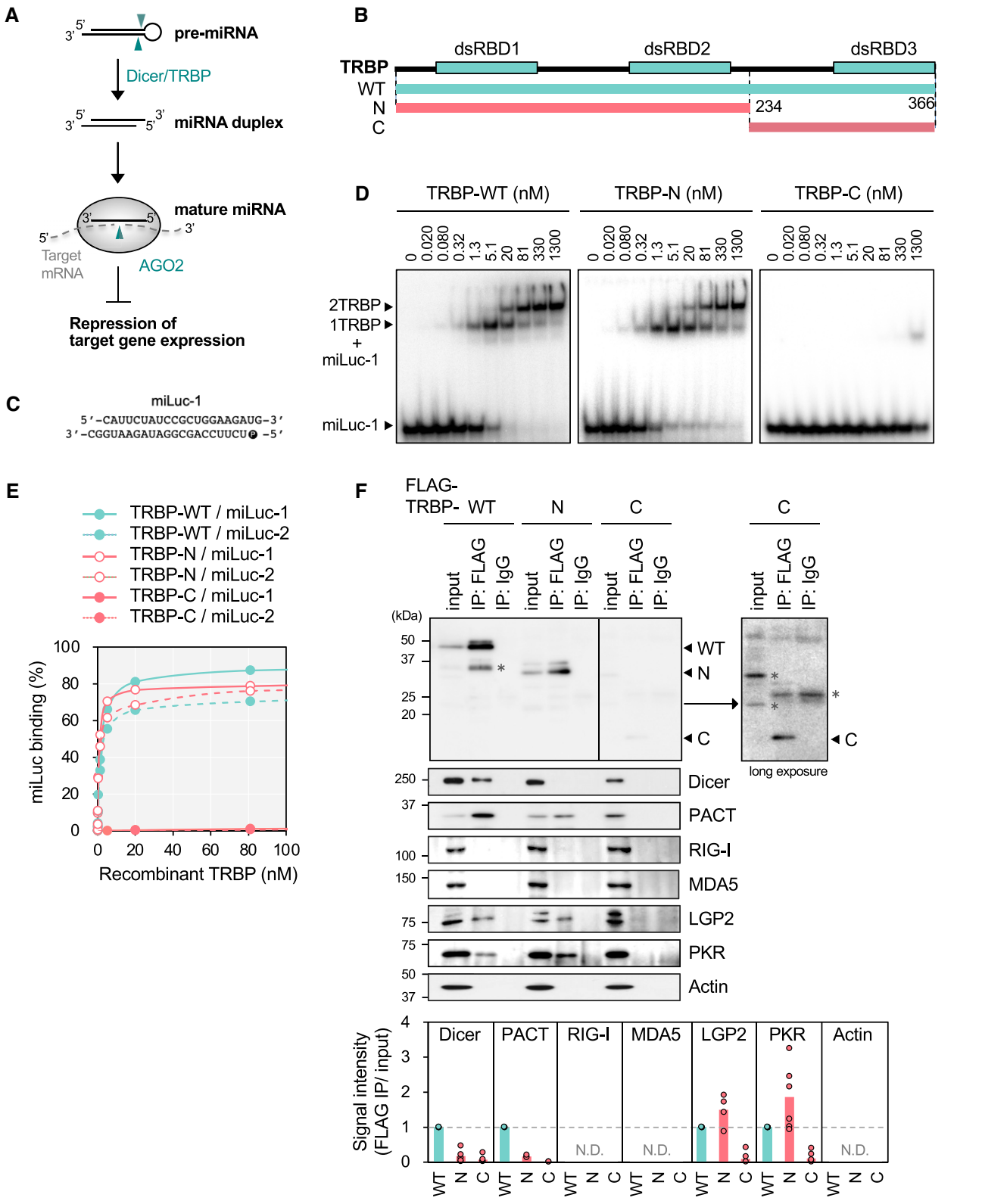

Figure 3. Processed TRBP interacts with IFN modulators but not with RNA-silencing factors. (**A**) Schematic of the pre-miRNA-mediated RNA-silencing pathway. (**B**) The domain structure of TRBP and the N- or C-terminal fragment of processed TRBP. (**C**) Sequence of miLuc-1. The guide strand was labeled with ^{32}P. (**D**) Electrophoresis mobility shift assay (EMSA) of TRBP-WT, N, or C with miLuc-1. ^{32}P-labeled miLuc-1 was incubated with increasing amounts of TRBP proteins and electrophoresed on a 9% polyacrylamide gel. Complex 1 is miLuc1 and monomeric TRBP-WT of the TRBP-N protein complex, and complex 2 is miLuc-1 and dimeric TRBP-WT of the TRBP-N protein complex. (**E**) dsRNA-binding activity of TRBP-WT, N and C by EMSA. Signal intensities were quantified by ImageQuant. (**F**) Immunoprecipitation of TRBP-WT, N and C. A plasmid encoding FLAG-tagged TRBP-WT, N or C was transfected into IFN-treated TRBP$^{-/-}$ cells, and immunoprecipitation was performed with an anti-FLAG antibody. Endogenous Dicer, PACT, RIG-I, MDA5, LGP2, PKR and actin were detected by Western blotting. Band intensities were quantified, and immunoprecipitation values were normalized to the input (FLAG/input). * indicates non-specific bands.

an enhanced ability to interact with PKR and LGP2. These results suggest that processing of TRBP changes its interaction partners from RNA-silencing factors to IFN regulators during viral infection.

Processed TRBP does not enhance RNA silencing during viral infection

Next, we performed luciferase reporter assays to evaluate the RNA-silencing activity of TRBP-WT, -N and -C in TRBP$^{-/-}$ cells (Figure 4A). A plasmid encoding a short-hairpin-structured RNA targeting firefly *luciferase* (pre-miLuc) was co-transfected with plasmids encoding the firefly *luciferase* gene and *Renilla luciferase* gene (internal control) into TRBP$^{-/-}$ cells. The cells were collected at 24 h following the transfection without SeV infection. The protein expression was confirmed by Western blot (Figure 4B) and the TRBP-C proteins did not express stably, consistent with Figure 3F. The cleavage of pre-miLuc by Dicer is necessary to silence the firefly *luciferase* gene (Figure 3A). Firefly luciferase activity was normalized to that of *Renilla* luciferase, and relative luciferase activity was calculated as firefly luciferase activity/*Renilla* luciferase activity. The expression of TRBP-WT decreased relative luciferase activity, whereas the expression of TRBP-N did not (Figure 4A), which suggests that full-length TRBP-WT is necessary for enhancing RNA-silencing activity. These results indicate that processing of TRBP abolishes its function as an enhancer of RNA silencing. To understand the role of TRBP in the maturation of miRNAs during viral infection, we performed small RNA sequencing of mock-treated or SeV-infected WT and TRBP$^{-/-}$ cells (Figure 4C). The cells were collected at 18 h following SeV infection. The XY plots showed that 85 or 115 mature miRNAs were downregulated by SeV infection in WT or TRBP$^{-/-}$ cells (SeV/mock < 0.5; Figure 4C and Supplementary Tables S4 and S5). The Venn diagram showed that 53 mature miRNAs were downregulated in both WT and TRBP$^{-/-}$ cells, and 32 and 62 mature miRNAs were downregulated in WT and TRBP$^{-/-}$ cells, specifically (Figure 4D). In our previous report, we identified 40 TRBP-bound pre-miRNAs by small RNA-seq of immunoprecipitated pre-miRNAs with TRBP using Flp-In 293 FLAG-TRBP cells (24). Among the 85 downregulated miRNAs in SeV-infected WT HeLa cells, 7 miRNAs (miR-345, 1304, 744, 25, 29c, 582 and 106b) were TRBP-bound miRNAs in Flp-In 293 FLAG-TRBP cells. Among them, the expression levels of six miRNAs except for miR-25 also decreased by SeV infection in TRBP$^{-/-}$ cells, indicating that most of the miRNAs downregulated by SeV are overlapped with TRBP-bound miRNAs, and the processed TRBP-N or -C cannot increase the mature miRNA levels during SeV infection. To investigate whether the processing of TRBP regulates the maturation of the downregulated miRNAs, such as miR-106b, by SeV infection, we transfected a plasmid encoding TRBP-WT or -D234A into TRBP$^{-/-}$ cells and collected cells at 24 following SeV infection. Western blot showed that TRBP-WT proteins but not TRBP-D234A proteins were processed by SeV infection, although the expression level of TRBP-D234A proteins might be slightly higher than that of TRBP-WT (Figure 4E). The qRT-PCR revealed that the mature miR-106b level decreased by SeV infection in TRBP-WT cells but not in TRBP-D234A cells (Figure 4F), indicating that the maturation of miR-106b is suppressed by TRBP processing. Thus, the full-length TRBP functions to enhance the maturation of miR-106b, and the processing of TRBP abolishes its ability to enhance its maturation.

Processing of TRBP enhances apoptosis via endoplasmic reticulum (ER) stress during SeV infection

Processing of TRBP abolished its interaction with Dicer (Figure 3F), which indicates a loss of its ability to enhance RNA silencing activities (Figure 4). Thus, processing of TRBP modulates gene expression directly or indirectly by repressing the maturation of TRBP-bound miRNAs during viral infection. To examine the effects of TRBP processing on the gene expression profile, we performed microarray analyses using mock-treated or SeV-infected TRBP$^{-/-}$ cells expressing TRBP-WT or -D234A without an epitope tag (TRBP-WT or -D234A cells) 24 h after infection. An XY plot showed that 222 and 182 transcripts were upregulated by SeV infection in TRBP-WT and -D234A cells, respectively (SeV/mock > 5; Figure 5A and C). GO analyses of the upregulated transcripts revealed that both were enriched in GO terms related to the antiviral innate immune response: type I interferon signaling pathway, defense response to virus, and negative regulation of viral genome replication (Figure 5B and D and Supplementary Tables S6 and S7). This indicates that induction of the innate immune response was unaffected by TRBP processing in both cell types. An XY plot showed that the gene expression profile of TRBP-WT cells was similar to that of TRBP-D234A cells without viral infection (Figure 5E, upper panel). By contrast, 200 transcripts were upregulated in SeV-infected TRBP-WT cells but not in SeV-infected TRBP-D234A cells (TRBP-WT/TRBP-D234A > 2) (Figure 5E, lower panel). Analyses of the cumulative distribution confirmed significant upregulation of the 200 transcripts by SeV infection in TRBP-WT cells (Supplementary Figure S11). GO analyses revealed that 200 transcripts were differentially upregulated in TRBP-WT cells compared to SeV-infected TRBP-D234A cells. These transcripts were enriched in GO terms related to ER stress, unfolded protein response (UPR), and apoptosis signaling: response to ER stress, intrinsic apoptotic signaling pathway in response to ER stress, protein folding, and inositol requiring 1 (IRE1)-mediated unfolded protein response (Figure 5F and Supplementary Table S8). qRT-PCR was used for validation of mRNA levels of MAP3K5 and TMBIM6, and confirmed that their mRNA levels were certainly upregulated in SeV-infected TRBP-WT cells compared with SeV-infected TRBP-D234A cells consistent with the microarray results (Figure 5G). In virus-infected cells, large amounts of viral proteins are synthesized, and unfolded or misfolded proteins accumulate in the ER (55). The accumulated proteins activate UPR signaling, and apoptosis is induced when ER stress is prolonged and the UPR fails to restore its homeostasis. Comparative analyses of the gene expression profiles of HeLa cells expressing TRBP-WT showed that levels of transcripts related to the GO term: response to ER stress (GO:0034976) in SeV-infected cells were higher at 24 h than those at 14 h (Figure 5H and Supplementary Figure S12), which suggests that SeV infection triggers prolonged ER stress. Levels of transcripts related to the GO term: UPR signaling (GO:0030968) were weakly upregulated during SeV infection (Figure 5H and Supplementary Figure S13), which suggests that by prolonging ER stress and activating UPR signaling, SeV infection promotes apoptosis. The expression of TRBP-N did not upregulate the transcripts

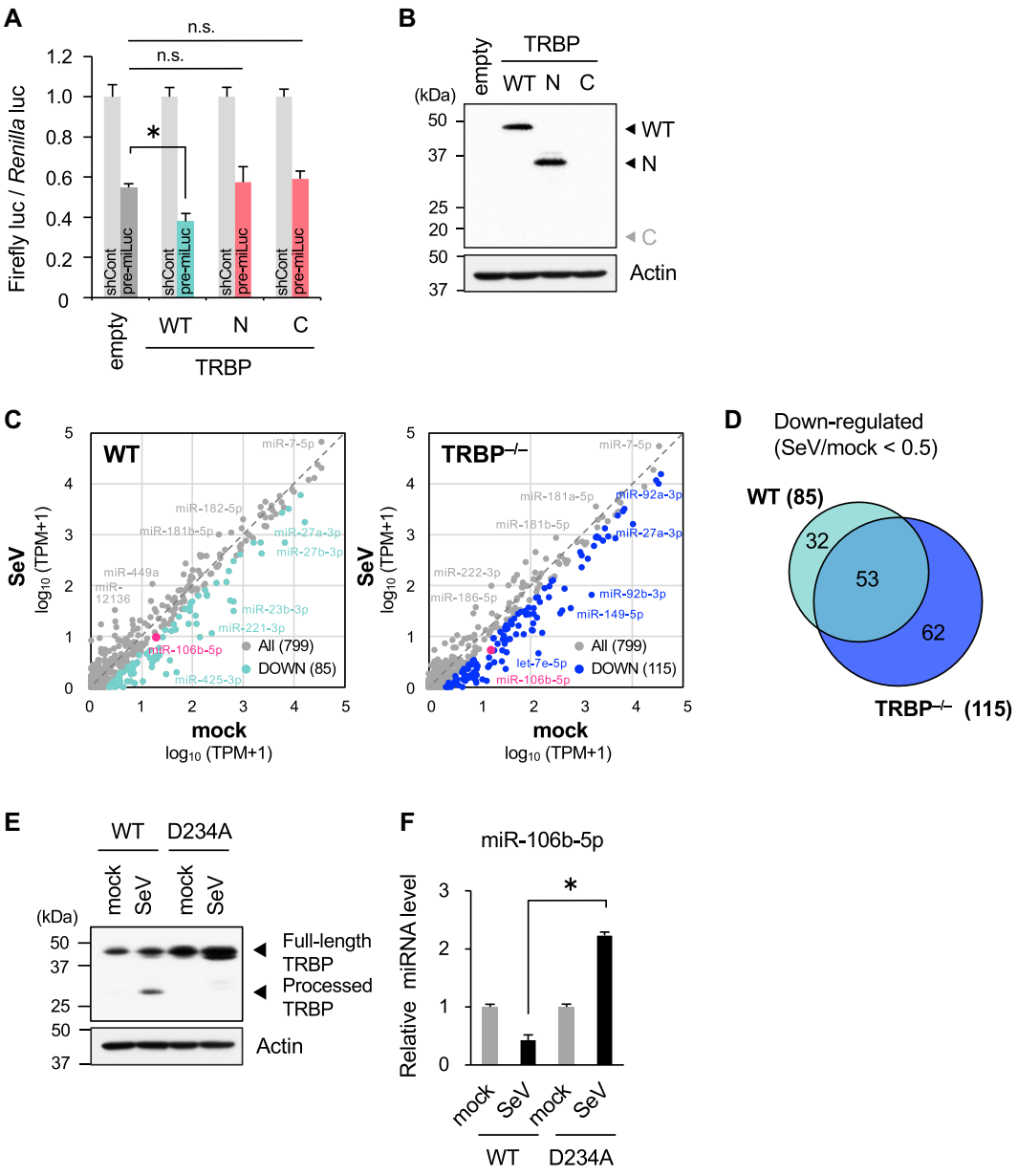

Figure 4. Processed TRBP does not enhance RNA silencing during viral infection. (**A**) RNA-silencing activity assay using a dual luciferase reporter in TRBP$^{-/-}$ cells transfected with empty vector or a plasmid encoding TRBP-WT, N or C. Plasmids encoding pre-miLuc targeting firefly luciferase or *Renilla* luciferase (internal control) were co-transfected; relative luciferase activity was calculated as firefly luciferase/*Renilla* luciferase. *P* values were determined by Student's *t* test (*$P < 0.05$). (**B**) Western blotting of TRBP$^{-/-}$ cells transfected with empty vector or a plasmid encoding TRBP-WT, -N, or -C. (**C**) XY plot of mature miRNAs expressed in mock-treated or SeV-infected WT or TRBP$^{-/-}$ cells. The cells were collected at 18 h following SeV infection and small RNA-seq was performed. (**D**) Venn diagram of mature miRNAs downregulated by SeV infection in WT or TRBP$^{-/-}$ cells. (**E**) Relative RNA levels of mature miR-106b in mock-treated or SeV infected TRBP$^{-/-}$ cells expressing TRBP-WT or -D234A as quantified by qRT-PCR. (**F**) Western blotting of mock-treated or SeV infected TRBP$^{-/-}$ cells expressing TRBP-WT or -D234A.

related to the response to ER stress (GO:0034976), UPR signaling (GO:0030968) and intrinsic apoptosis signaling pathway in response to ER stress (GO:0070059) in non-virus-infected cells (Supplementary Figure S14), indicating that the TRBP-N protein itself does not induce the upregulation of these genes.

To verify that processing of TRBP regulates apoptosis, we transfected a plasmid encoding TRBP-WT or -D234A into TRBP$^{-/-}$ cells and detected apoptotic cell death using Annexin V for 24 h after SeV infection (Figure 6). The empty plasmid was used as a control of the transfection. Western blots showed that TRBP-WT proteins but not TRBP-D234A proteins were processed by SeV infection (Figure 6A), suggesting that the effect of this processing on apoptosis can be evaluated by comparing the results between TRBP-WT and -D234A. The percentages of apoptotic cell death of the cells transfected with TRBP-WT- and TRBP-D234A-encoding plasmid were 28.6 ± 4.59% and 21.6 ± 2.19%, respectively (Figure 6B), indicating that the processing of TRBP enhances the apoptosis of virus-infected cells. Furthermore, qRT-PCR for SeV phosphoprotein (P) gene was performed to measure intracellular viral RNA levels (Figure 6C). The results demonstrated that TRBP-WT decreased viral RNA levels in the cells compared with TRBP-D234A. These results indicate that apoptosis was

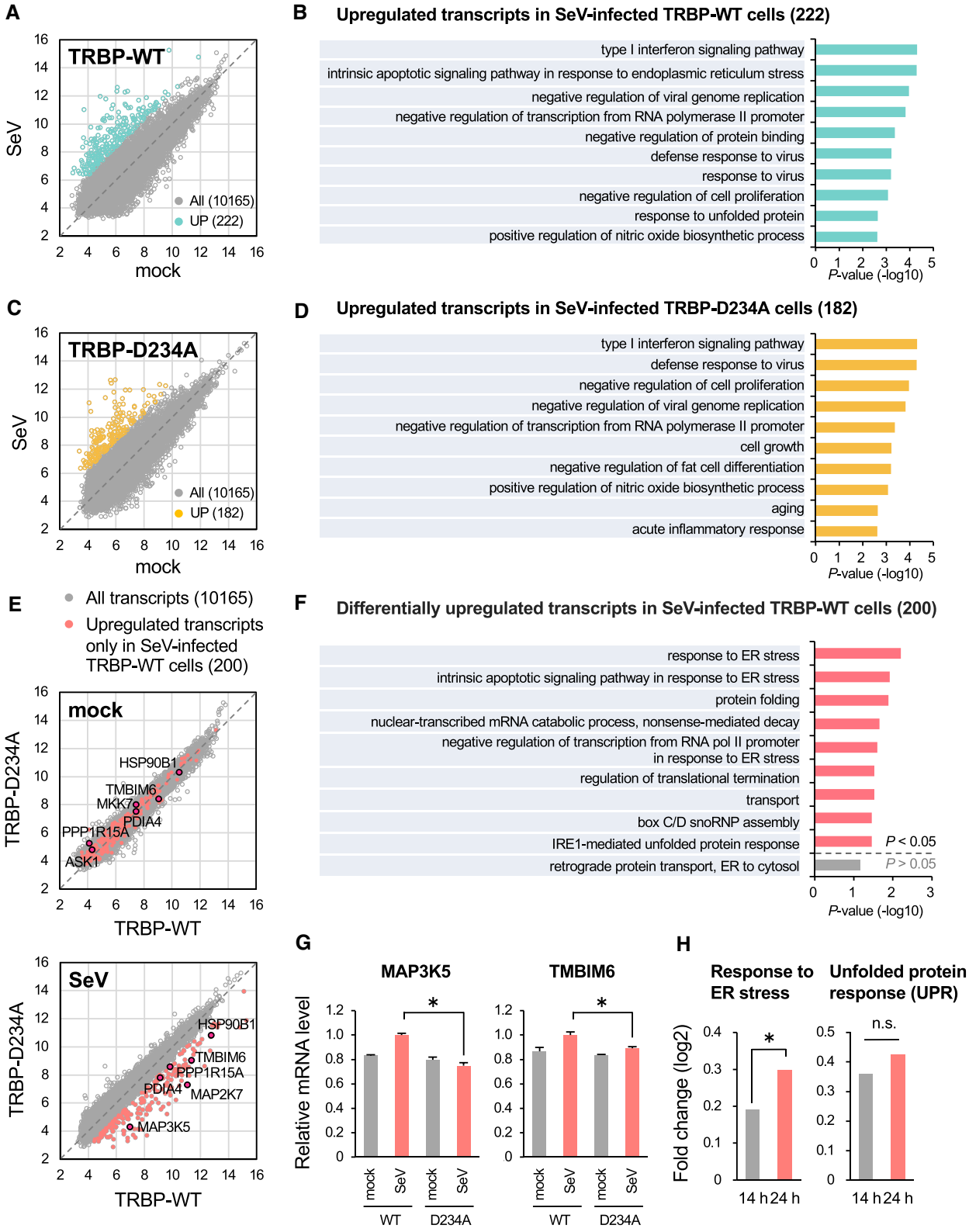

Figure 5. Processed TRBP enhances apoptosis during SeV infection. (**A**) XY plot of microarray signals of all transcripts expressed in mock-treated or SeV-infected TRBP-WT cells. Green, transcripts upregulated by SeV infection (SeV/mock > 5). (**B**) Gene ontology analysis of upregulated transcripts in SeV-infected TRBP-WT cells. (**C**) XY plot of microarray signals of all transcripts expressed in mock-treated or SeV-infected TRBP-D234A cells. Yellow, transcripts upregulated by SeV infection (SeV/mock > 5). (**D**) Gene ontology analysis of upregulated transcripts in SeV-infected TRBP-D234A cells. (**E**) XY plots of microarray signals of all transcripts in mock-treated or SeV-infected TRBP-WT or D234A cells. Pink, transcripts upregulated by SeV infection only in TRBP-WT cells. (**F**) Gene ontology analysis of transcripts upregulated only in SeV-infected TRBP-WT cells. (**G**) Relative RNA levels of MAP3K5 and TMBMI6 in mock-treated or SeV infected TRBP-WT or -D234A cells (**H**) Differences in the integral values of cumulative distribution between all transcripts and those related to the response to ER stress (GO:0034976) or unfolded stress response (GO:0030968) 14 or 24 h following SeV infection.

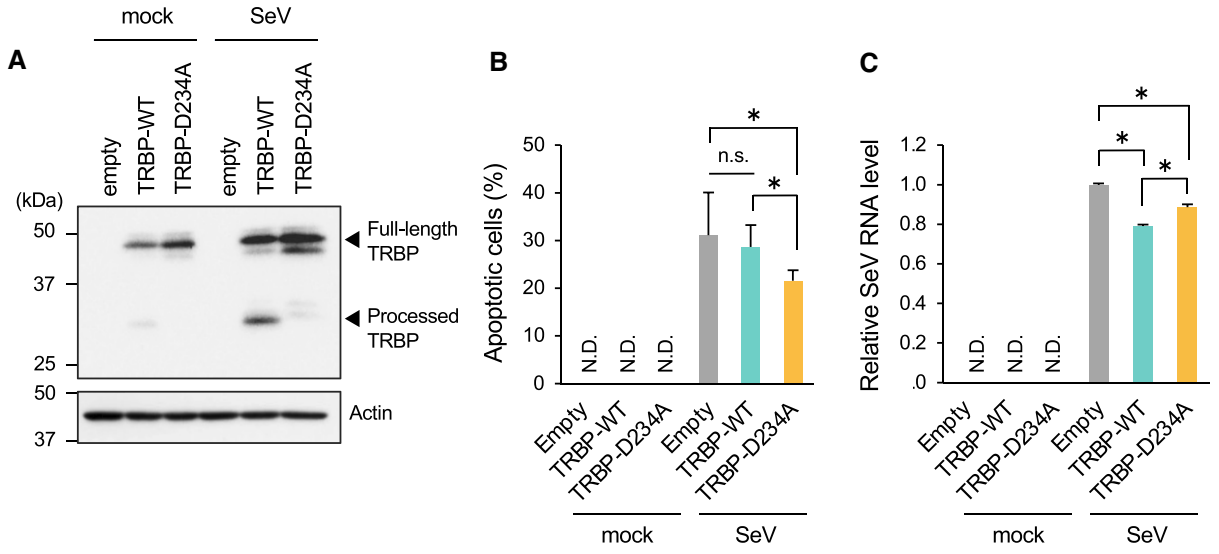

Figure 6. Processing of TRBP enhances apoptosis of virus-infected cells. (**A**) Western blotting of mock-treated or SeV-infected TRBP$^{-/-}$ cells transfected an empty vector or plasmid encoding TRBP-WT or D234A. The cells were collected at 24 following SeV infection. (**B**) Ratio of apoptotic cells of mock-treated or SeV-infected TRBP$^{-/-}$ cells transfected an empty vector or plasmid encoding TRBP-WT or D234A. (**C**) Relative RNA levels of SeV RNA of P gene quantified by qRT-PCR.

enhanced and viral RNA levels might be repressed when TRBP was processed in virus-infected cells.

Processed TRBP represses IFN production during viral infection

Processed N-terminal TRBP did not interact with Dicer and PACT (RNA-silencing factors) but interacted with PKR and LGP2 (IFN modulators; Figure 3F). TRBP enhances RNA silencing in non-virus-infected cells but might be converted into an IFN modulator through inducing ER stress by processing induced by viral infection. To investigate whether TRBP regulates IFN production, we performed qRT-PCR to measure IFN levels in TRBP$^{-/-}$ cells collected 0, 6, 10, 14, 18 and 24 h after SeV infection (Supplementary Figure S15). SeV infection induced IFN production, which peaked 6 h after infection and decreased rapidly thereafter. This is likely because prolonged overproduction of IFN induces an excessive immune response, possibly leading to autoimmune disorders (56). To investigate whether processed TRBP regulates IFN production, we transfected cells with plasmids expressing TRBP-WT, -N, -C or -D234A and harvested them 6, 18 and 24 h after SeV infection (Figure 7). Western blots showed that TRBP-WT proteins were processed at 18 h and 24 h but not at 6 h (Figure 7A–C). TRBP-C proteins were not expressed stably consistent with Figure 3F and not decreased the IFN production at any time points. qRT-PCR showed that the expression of TRBP-WT did not decrease IFN production at 6 h but decreased at 18 h and 24 h, whereas IFN levels were already decreased at 6 h by TRBP-N expression (Figure 7D-F). Furthermore, the expression of TRBP-WT and -N decreased the IFN production more strongly than TRBP-D234A at 18 h. The protein level of TRBP-D234A appeared slightly elevated compared to TRBP-WT and -N (Figure 7A-C). The probable explanation for this can be attributed to the instability observed not only in the processed TRBP -C, as shown in Figure 3F, but also slight instability in TRBP -N, compared to that of the unprocessed TRBP-D234A protein. These findings indicate that processed TRBP likely plays a role in suppressing IFN production.

Discussion

We report functional conversion of TRBP during viral infection (Figure 8). TRBP is an enhancer of RNA silencing that, in collaboration with Dicer, targets the processing of a subset of miRNAs in non-virus-infected cells. By contrast, in virus-infected cells, TRBP induces apoptosis irreversibly, possibly suppressing the IFN response induced by viral infection.

In the early stage of viral infection, apoptosis is induced by the interaction of TRBP with a virus sensor protein, LGP2 (24). The expression of LGP2 is low in non-virus-infected cells but is increased by a positive feedback loop involving secreted IFN during viral infection. The expression of LGP2 increases 10 and 14 h after SeV infection (42), and LGP2 interacts with TRBP to inhibit the function as an RNA silencing enhancer through the competitive interaction against pre-miRNAs (24). Then, we revealed that apoptosis is induced by upregulation of apoptosis-inducing factors by inhibiting the maturation of the specific types of miRNAs.

In the late stage of viral infection, TRBP enhances apoptosis (Figure 6), which may repress the IFN response (Figure 7). Infection by NDV or SeV, but not IAV, induces the activation of caspases (Figure 1). Caspase-3 processes TRBP at a position in the linker region between dsRBD2 and dsRBD3 18 h after viral infection (Figure 2). The processing divides TRBP into two fragments, TRBP-N and TRBP-C; TRBP-N binds to pre-miRNA but does not interact with Dicer (Figure 3). Neither fragment enhances RNA silencing (Figure 4), which indicates that processed TRBP does not function as an enhancer of RNA silencing. TRBP-N is capable to bind miRNAs (Figure 3) but did not repress RNA silencing in this condition. We do not exclude the possibility that TRBP-N might function in dominant negative manner in different conditions.

In the later stage of viral infection, large amounts of viral proteins are synthesized, and unfolded or misfolded proteins accumulate in the ER (55), triggering the UPR. When a cell is unable to recover from ER stress, apoptosis is induced. In this study, processed TRBP induced the upregulation of ER- and UPR-related genes. Therefore, the interaction of TRBP-N with

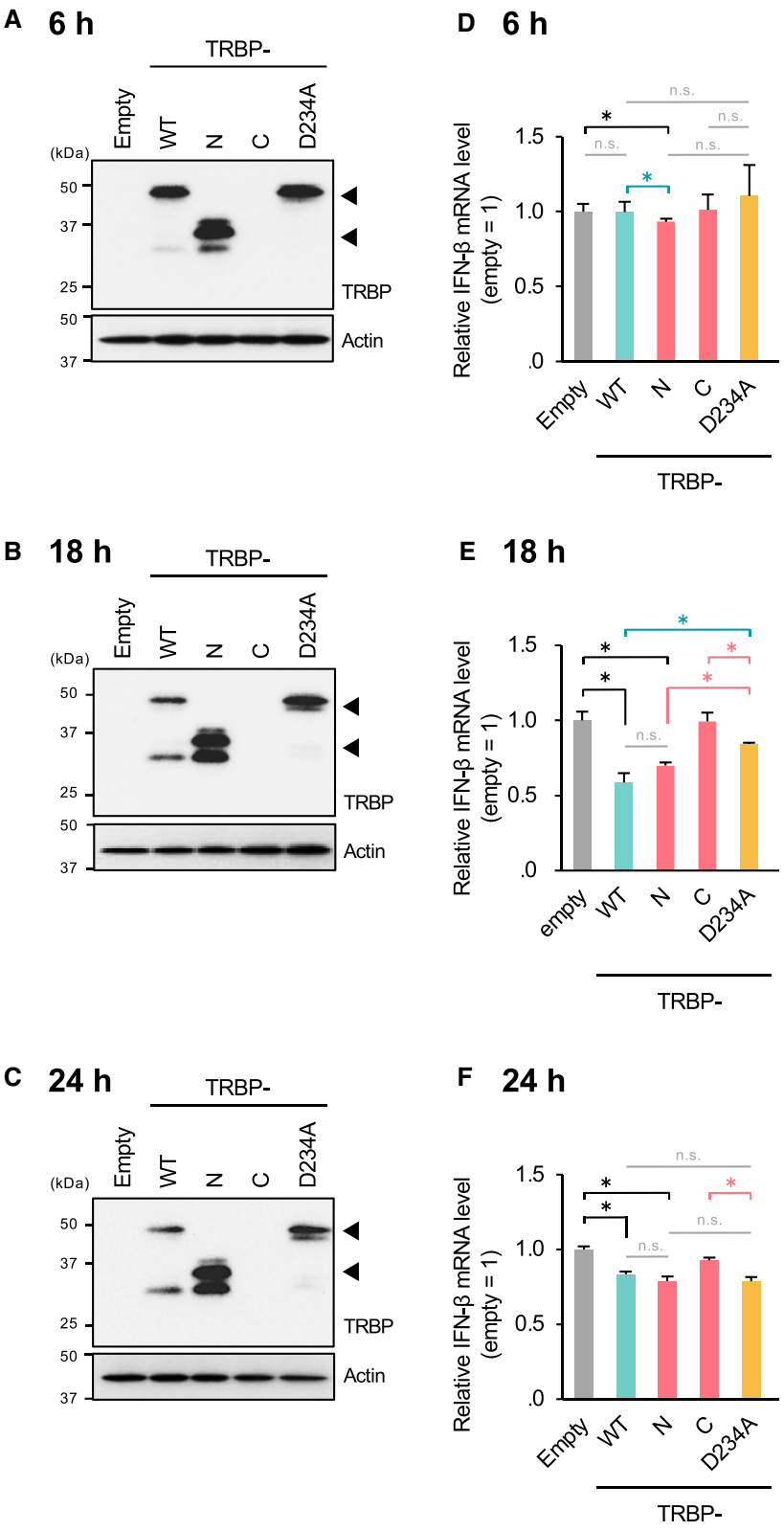

Figure 7. Processed TRBP represses IFN production during viral infection. Western blotting (**A**–**C**) and relative mRNA levels (**D**–**F**) of SeV-infected TRBP$^{-/-}$ cells transfected with empty vector or a plasmid encoding TRBP-WT, -N, -C, -D234A, or -dsRBDmt1 + 2. Cells were collected at 6 h (A, D), 18 h (B, E), 24 h (C, F) following infection.

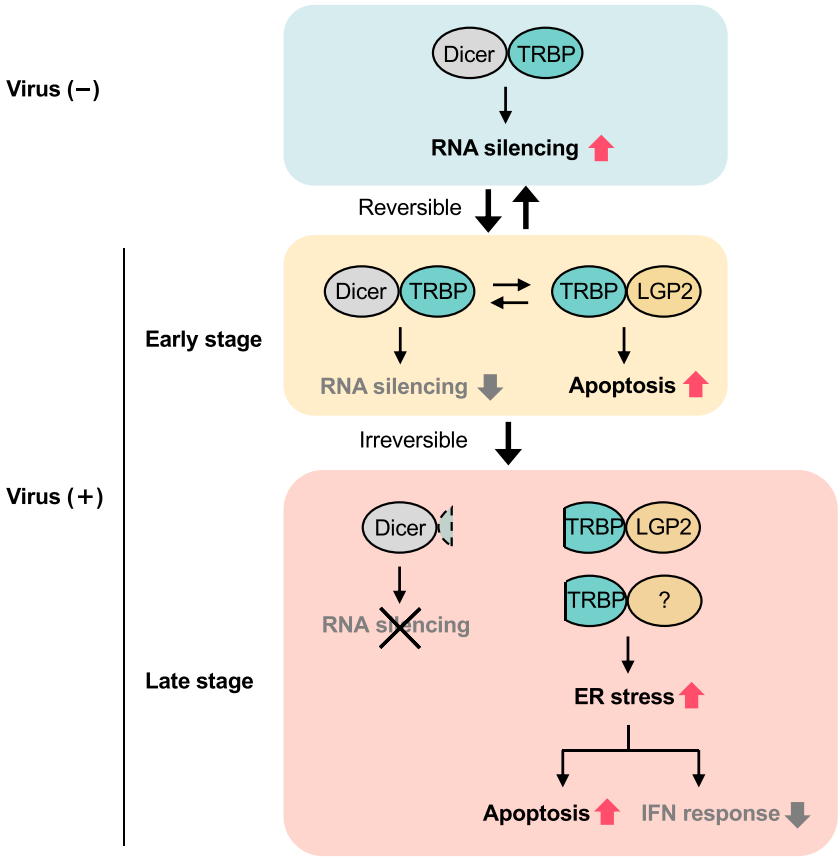

Figure 8. TRBP functions in both RNA silencing and the IFN response during viral infection. (Upper panel) TRBP enhances RNA silencing by interacting with Dicer in non-virus-infected cells. (Middle panel) In the early stage of viral infection, the interaction of TRBP with LGP2 is enhanced, but the interaction of TRBP with Dicer is suppressed. The TRBP–LGP2 interaction upregulates apoptosis-regulatory genes, whereas suppression of the TRBP–Dicer interaction decreases RNA-silencing activity. (Lower panel) In the late stage of SeV infection, the activation of caspases triggers the processing of TRBP. Processed TRBP does not interact with Dicer and does not function as an enhancer of RNA silencing. However, processed TRBP interacts with LGP2 or some other as-yet-unidentified factor, thereby enhancing ER stress-trigged apoptosis and repressing the IFN response.

LGP2 or other IFN-inducible unidentified factors may induce ER stress in SeV-infected cells, irreversibly inducing apoptosis.

TRBP-WT and N repress IFN production during SeV infection (Figure 7). SeV is recognized by RIG-I, resulting in IFN production (18). RIG-I interacts with LGP2 when both are expressed at a high level (57), but the role of LGP2 in IFN signaling is unclear. Some studies (58,59) have indicated that LGP2 enhances the activation of RIG-I, whereas others have reported a suppressive effect (60,61). In this study, immunoprecipitation showed that LGP2 and PKR interact more strongly with TRBP-N than with TRBP-WT (Figure 3). Therefore, loss of the interaction with Dicer caused by the processing of the C-terminal domain may eliminate the steric hindrance of the interaction of TRBP with LGP2 or PKR. TRBP is a repressor of PKR (62). PKR is activated by exogenous dsRNAs, including viral RNAs, and induces global translational repression to suppress viral replication by phosphorylating the alpha subunit of eIF2 (eIF2α). However, the C protein of SeV represses the activation of PKR (42,63), which suggests that TRBP regulates IFN production independently of its interaction with PKR during SeV infection. By contrast, infection by NDV induces the activation of PKR (42,64). Active PKR globally represses translation such that the protein level of LGP2 is not increased. TRBP may interact with PKR but not LGP2 and function as a PKR repressor during NDV infection. However, SeV infection does not activate PKR. Therefore, some other protein kinase, such as PKR-like ER kinase (PERK), may phosphorylate eIF2α during SeV infection; indeed, PERK is activated by ER stress (55). Thus, the phosphorylation of eIF2α may be induced not only by activation of PKR but also by the ER stress induced by the accumulation of viral proteins in the ER during SeV infection.

IFN production is strictly regulated, and prolonged overproduction of IFN induces an excessive immune response. Processed TRBP may prevent the overproduction of IFN after its peak during viral infection. Apoptosis of SeV-infected cells is induced by the repression of TRBP-bound miRNAs via the interaction with LGP2 14 h after SeV infection (24,42). LGP2 is an RLR that modulates RNA silencing during viral infection and upregulates apoptosis-regulatory genes, including those encoding caspases (24,42). Here we found that TRBP is processed by caspase(s) >18 h after SeV infection, which enhances apoptosis by inducing ER stress (Figure 6). Thus, in the early stage of viral infection, the induction of apoptosis may be reversible. However, in the late stage, apoptosis is induced via an irreversible mechanism that may repress the IFN response, potentially preventing autoimmunity. SeV infection induces apoptosis, but possibly not in all cell types.

Several regulatory mechanisms of RNA-silencing factors have been reported. Dicer is cleaved by caspases during apoptosis triggered by TNFα and other stress stimuli (65). Multiple RNA-silencing factors (Drosha, DGCR8, Dicer, and TRBP)

are cleaved by caspases in heat-shocked cells, an effect inhibited by the overexpression of HSP70 (66). In this study, Dicer cleavage was not triggered by viral infection, poly(I:C) transfection, or TNFα/CHX treatment, and the expression of full-length Dicer was unaffected by these stimuli (Figure 1). By contrast, NDV or SeV infection, poly(I:C) transfection, and TNFα/CHX treatment triggered the processing of TRBP, the function of which was altered to that of an IFN repressor (Figure 8). The expression of full-length TRBP was decreased and that of processed TRBP was increased by these stimuli. However, the processed TRBP-N and TRBP-C fragments may have different stabilities. We purified recombinant TRBP-WT, N and C from *E. coli* (Supplementary Figure S7), but TRBP-C was slightly detectable or undetectable by Western blotting using cell lysate (Figure 3). The mRNAs of TRBP-C, WT, and N were detected by RT-PCR (Supplementary Figure S9), which indicates that TRBP-C protein is unstable. The C-terminal region of TRBP is ubiquitinated by Merlin (encoded by *Nf2*) (67). The expression of Merlin facilitates the degradation of TRBP-WT but not TRBP-ΔdsRBD3 via the ubiquitin-proteasome pathway (67), which suggests that Merlin facilitates the degradation of TRBP-C.

The TRBP amino acid sequence is conserved in mammalian, but not non-mammalian, genomes (Supplementary Figures S16–S18). Several amino acids are substituted but the DARD/G-processing motif is conserved completely in several mammalian genomes (Supplementary Figure S16). RNA silencing is induced by endogenous miRNAs, and IFN signaling is activated by exogenous viral RNAs. RNA silencing and IFN signaling were formerly considered independent pathways, but multiple reports, including ours, have demonstrated crosstalk between them (24,25,42,57,68–72). In the early stage of viral infection of mammalian cells, TRBP functions as a hub between RNA silencing and IFN signaling by interacting with LGP2 rather than Dicer (Figure 8). After processing, TRBP enhances apoptosis irreversibly in the late stage of viral infection. These studies indicate that TRBP is a multifunctional protein in RNA silencing and IFN signaling during viral infection in mammalian cells.

Data availability

The microarray data underlying this article is available at https://www.ncbi.nlm.nih.gov/geo/ under accession code GSE234550. RNA-sequence data is available in the DDBJ Sequence Read Archive of the National Institute of Genetics, Japan, under accession code PRJDB17739.

Supplementary data

Supplementary Data are available at NAR Online.

Acknowledgements

T.T. and K.U.-T. designed the study at first, and T.T., K.S., H.M., K.O., Y.K., M.Y. and K.U.-T. discussed the methods, results and the experimental plans. T.T., K.S. H.M, K.O. and Y.K. performed the experiments, and T.T. analyzed small RNA-seq and microarray data. T.M. and M.T. performed N-terminal amino acid sequencing. The manuscript was drafted by T.T. and K.U.-T., and T.T., M.Y. and K.U.-T. were involved in reviewing the manuscript. All authors read and approved the final manuscript. We would like to express our gratitude to Dr K. Saigo for his valuable discussions on this study.

Funding

Ministry of Education, Culture, Sports, Science and Technology of Japan [21310123, 21115004, 15H04319, 16H14640, 221S0002, 16H06279 to K.U.-T., 15K19124, 18K15178 to T.T.]; SECOM Science and Technology Foundation; Takeda Science Foundation; MSD Life Science Foundation; Naito Science & Engineering Foundation; Canon Foundation (to T.T.); Japan Health & Research Institute and the Kurata Grant awarded by the Hitachi Global Foundation to K.U.-T.); Joint Usage/Research Program of Medical Mycology Research Center, Chiba University [14-14, 15-16, 16-1, 17-15, 18-11, 19-1, 20-1, 21-05, 22-04, 23-04, 24-04 to T.T., K.O., M.Y., K.U.-T.]. Funding for open access charge: The Ministry of Education, Culture, Sports, Science and Technology of Japan.

Conflict of interest statement

None declared.

References

1. Kozomara,A. and Griffiths-Jones,S. (2014) miRBase: annotating high confidence microRNAs using deep sequencing data. *Nucleic Acids Res.*, **42**, D68–D73.
2. Lee,Y., Ahn,C., Han,J., Choi,H., Kim,J., Yim,J., Lee,J., Provost,P., Rådmark,O., Kim,S., *et al.* (2003) The nuclear RNase III Drosha initiates microRNA processing. *Nature*, **425**, 415–419.
3. Gregory,R.I., Yan,K.P., Amuthan,G., Chendrimada,T., Doratotaj,B., Cooch,N. and Shiekhattar,R. (2004) The microprocessor complex mediates the genesis of microRNAs. *Nature*, **432**, 235–240.
4. Denli,A.M., Tops,B.B., Plasterk,R.H., Ketting,R.F. and Hannon,G.J. (2004) Processing of primary microRNAs by the microprocessor complex. *Nature*, **432**, 231–235.
5. Han,J., Lee,Y., Yeom,K.H., Kim,Y.K., Jin,H. and Kim,V.N. (2004) The Drosha-DGCR8 complex in primary microRNA processing. *Genes Dev.*, **18**, 3016–3027.
6. Han,J., Lee,Y., Yeom,K.H., Nam,J.W., Heo,I., Rhee,J.K., Sohn,S.Y., Cho,Y., Zhang,B.T. and Kim,V.N. (2006) Molecular basis for the recognition of primary microRNAs by the Drosha-DGCR8 complex. *Cell*, **125**, 887–901.
7. Yi,R., Qin,Y., Macara,I.G. and Cullen,B.R. (2003) Exportin-5 mediates the nuclear export of pre-microRNAs and short hairpin RNAs. *Genes Dev.*, **17**, 3011–3016.
8. Lund,E., Güttinger,S., Calado,A., Dahlberg,J.E. and Kutay,U. (2004) Nuclear export of microRNA precursors. *Science*, **303**, 95–98.
9. Doi,N., Zenno,S., Ueda,R., Ohki-Hamazaki,H., Ui-Tei,K. and Saigo,K. (2003) Short-interfering-RNA-mediated gene silencing in mammalian cells requires Dicer and eIF2C translation initiation factors. *Curr. Biol.*, **13**, 41–46.
10. Liu,J., Carmell,M.A., Rivas,F.V., Marsden,C.G., Thomson,J.M., Song,J.J., Hammond,S.M., Joshua-Tor,L. and Hannon,G.J. (2004) Argonaute2 is the catalytic engine of mammalian RNAi. *Science*, **305**, 1437–1441.
11. Rivas,F.V., Tolia,N.H., Song,J.J., Aragon,J.P., Liu,J., Hannon,G.J. and Joshua-Tor,L. (2005) Purified Argonaute2 and an siRNA form recombinant human RISC. *Nat. Struct. Mol. Biol.*, **12**, 340–349.
12. Matranga,C., Tomari,Y., Shin,C., Bartel,D.P. and Zamore,P.D. (2005) Passenger-strand cleavage facilitates assembly of siRNA into Ago2-containing RNAi enzyme complexes. *Cell*, **123**, 607–620.

13. Meister,G., Landthaler,M., Peters,L., Chen,P.Y., Urlaub,H., Lührmann,R. and Tuschl,T. (2005) Identification of novel argonaute-associated proteins. *Curr. Biol.*, **15**, 2149–2155.
14. Jakymiw,A., Lian,S., Eystathioy,T., Li,S., Satoh,M., Hamel,J.C., Fritzler,M.J. and Chan,E.K. (2005) Disruption of GW bodies impairs mammalian RNA interference. *Nat. Cell Biol.*, **7**, 1267–1274.
15. Liu,J., Valencia-Sanchez,M.A., Hannon,G.J. and Parker,R. (2005) MicroRNA-dependent localization of targeted mRNAs to mammalian P-bodies. *Nat. Cell Biol.*, **7**, 719–723.
16. Behm-Ansmant,I., Rehwinkel,J., Doerks,T., Stark,A., Bork,P. and Izaurralde,E. (2006) mRNA degradation by miRNAs and GW182 requires both CCR4:NOT deadenylase and DCP1:DCP2 decapping complexes. *Genes Dev.*, **20**, 1885–1898.
17. Alexopoulou,L., Holt,A.C., Medzhitov,R. and Flavell,R.A. (2001) Recognition of double-stranded RNA and activation of NF-kappaB by Toll-like receptor 3. *Nature*, **413**, 732–738.
18. Yoneyama,M., Kikuchi,M., Natsukawa,T., Shinobu,N., Imaizumi,T., Miyagishi,M., Taira,K., Akira,S. and Fujita,T. (2004) The RNA helicase RIG-I has an essential function in double-stranded RNA-induced innate antiviral responses. *Nat. Immunol.*, **5**, 730–737.
19. Kawai,T. and Akira,S. (2009) The roles of TLRs, RLRs and NLRs in pathogen recognition. *Int. Immunol.*, **21**, 317–337.
20. Novick,D., Cohen,B. and Rubinstein,M. (1994) The human interferon alpha/beta receptor: characterization and molecular cloning. *Cell*, **77**, 391–400.
21. Sato,M., Hata,N., Asagiri,M., Nakaya,T., Taniguchi,T. and Tanaka,N. (1998) Positive feedback regulation of type I IFN genes by the IFN-inducible transcription factor IRF-7. *FEBS Lett.*, **441**, 106–110.
22. Marié,I., Durbin,J.E. and Levy,D.E. (1998) Differential viral induction of distinct interferon-alpha genes by positive feedback through interferon regulatory factor-7. *EMBO J.*, **17**, 6660–6669.
23. Yoneyama,M., Kikuchi,M., Matsumoto,K., Imaizumi,T., Miyagishi,M., Taira,K., Foy,E., Loo,Y.M., Gale,M., Akira,S., *et al.* (2005) Shared and unique functions of the DExD/H-box helicases RIG-I, MDA5, and LGP2 in antiviral innate immunity. *J. Immunol.*, **175**, 2851–2858.
24. Takahashi,T., Nakano,Y., Onomoto,K., Murakami,F., Komori,C., Suzuki,Y., Yoneyama,M. and Ui-Tei,K. (2018) LGP2 virus sensor regulates gene expression network mediated by TRBP-bound microRNAs. *Nucleic Acids Res.*, **46**, 9134–9147.
25. Takahashi,T. and Ui-Tei,K. (2020) Mutual regulation of RNA silencing and the IFN response as an antiviral defense system in mammalian cells. *Int. J. Mol. Sci.*, **21**, 1348.
26. Hornung,V., Ellegast,J., Kim,S., Brzózka,K., Jung,A., Kato,H., Poeck,H., Akira,S., Conzelmann,K.K., Schlee,M., *et al.* (2006) 5′-Triphosphate RNA is the ligand for RIG-I. *Science*, **314**, 994–997.
27. Pichlmair,A., Schulz,O., Tan,C.P., Näslund,T.I., Liljeström,P., Weber,F. and Reis e Sousa,C. (2006) RIG-I-mediated antiviral responses to single-stranded RNA bearing 5′-phosphates. *Science*, **314**, 997–1001.
28. Takahasi,K., Yoneyama,M., Nishihori,T., Hirai,R., Kumeta,H., Narita,R., Gale,M., Inagaki,F. and Fujita,T. (2008) Nonself RNA-sensing mechanism of RIG-I helicase and activation of antiviral immune responses. *Mol. Cell*, **29**, 428–440.
29. Wang,Y., Ludwig,J., Schuberth,C., Goldeck,M., Schlee,M., Li,H., Juranek,S., Sheng,G., Micura,R., Tuschl,T., *et al.* (2010) Structural and functional insights into 5′-ppp RNA pattern recognition by the innate immune receptor RIG-I. *Nat. Struct. Mol. Biol.*, **17**, 781–787.
30. Jiang,F., Ramanathan,A., Miller,M.T., Tang,G.Q., Gale,M., Patel,S.S. and Marcotrigiano,J. (2011) Structural basis of RNA recognition and activation by innate immune receptor RIG-I. *Nature*, **479**, 423–427.
31. Kowalinski,E., Lunardi,T., McCarthy,A.A., Louber,J., Brunel,J., Grigorov,B., Gerlier,D. and Cusack,S. (2011) Structural basis for the activation of innate immune pattern-recognition receptor RIG-I by viral RNA. *Cell*, **147**, 423–435.
32. Goubau,D., Schlee,M., Deddouche,S., Pruijssers,A.J., Zillinger,T., Goldeck,M., Schuberth,C., Van der Veen,A.G., Fujimura,T., Rehwinkel,J., *et al.* (2014) Antiviral immunity via RIG-I-mediated recognition of RNA bearing 5′-diphosphates. *Nature*, **514**, 372–375.
33. Kato,H., Takeuchi,O., Mikamo-Satoh,E., Hirai,R., Kawai,T., Matsushita,K., Hiiragi,A., Dermody,T.S., Fujita,T. and Akira,S. (2008) Length-dependent recognition of double-stranded ribonucleic acids by retinoic acid-inducible gene-I and melanoma differentiation-associated gene 5. *J. Exp. Med.*, **205**, 1601–1610.
34. Peisley,A., Lin,C., Wu,B., Orme-Johnson,M., Liu,M., Walz,T. and Hur,S. (2011) Cooperative assembly and dynamic disassembly of MDA5 filaments for viral dsRNA recognition. *Proc. Natl. Acad. Sci. U.S.A.*, **108**, 21010–21015.
35. Peisley,A., Jo,M.H., Lin,C., Wu,B., Orme-Johnson,M., Walz,T., Hohng,S. and Hur,S. (2012) Kinetic mechanism for viral dsRNA length discrimination by MDA5 filaments. *Proc. Natl. Acad. Sci. U.S.A.*, **109**, E3340–E3349.
36. Wu,B., Peisley,A., Richards,C., Yao,H., Zeng,X., Lin,C., Chu,F., Walz,T. and Hur,S. (2013) Structural basis for dsRNA recognition, filament formation, and antiviral signal activation by MDA5. *Cell*, **152**, 276–289.
37. Chendrimada,T.P., Gregory,R.I., Kumaraswamy,E., Norman,J., Cooch,N., Nishikura,K. and Shiekhattar,R. (2005) TRBP recruits the Dicer complex to Ago2 for microRNA processing and gene silencing. *Nature*, **436**, 740–744.
38. Haase,A.D., Jaskiewicz,L., Zhang,H., Lainé,S., Sack,R., Gatignol,A. and Filipowicz,W. (2005) TRBP, a regulator of cellular PKR and HIV-1 virus expression, interacts with Dicer and functions in RNA silencing. *EMBO Rep.*, **6**, 961–967.
39. Laraki,G., Clerzius,G., Daher,A., Melendez-Peña,C., Daniels,S. and Gatignol,A. (2008) Interactions between the double-stranded RNA-binding proteins TRBP and PACT define the Medipal domain that mediates protein-protein interactions. *RNA Biol.*, **5**, 92–103.
40. Daniels,S.M., Melendez-Peña,C.E., Scarborough,R.J., Daher,A., Christensen,H.S., El Far,M., Purcell,D.F., Lainé,S. and Gatignol,A. (2009) Characterization of the TRBP domain required for dicer interaction and function in RNA interference. *BMC Mol. Biol.*, **10**, 38.
41. Takahashi,T., Miyakawa,T., Zenno,S., Nishi,K., Tanokura,M. and Ui-Tei,K. (2013) Distinguishable in vitro binding mode of monomeric TRBP and dimeric PACT with siRNA. *PLoS One*, **8**, e63434.
42. Takahashi,T., Nakano,Y., Onomoto,K., Yoneyama,M. and Ui-Tei,K. (2020) LGP2 virus sensor enhances apoptosis by upregulating apoptosis regulatory genes through TRBP-bound miRNAs during viral infection. *Nucleic Acids Res.*, **48**, 1494–1507.
43. Daher,A., Laraki,G., Singh,M., Melendez-Peña,C.E., Bannwarth,S., Peters,A.H., Meurs,E.F., Braun,R.E., Patel,R.C. and Gatignol,A. (2009) TRBP control of PACT-induced phosphorylation of protein kinase R is reversed by stress. *Mol. Cell. Biol.*, **29**, 254–265.
44. Narita,R., Takahasi,K., Murakami,E., Hirano,E., Yamamoto,S.P., Yoneyama,M., Kato,H. and Fujita,T. (2014) A novel function of human Pumilio proteins in cytoplasmic sensing of viral infection. *PLoS Pathog.*, **10**, e1004417.
45. Ui-Tei,K., Naito,Y., Takahashi,F., Haraguchi,T., Ohki-Hamazaki,H., Juni,A., Ueda,R. and Saigo,K. (2004) Guidelines for the selection of highly effective siRNA sequences for mammalian and chick RNA interference. *Nucleic Acids Res.*, **32**, 936–948.
46. Onomoto,K., Jogi,M., Yoo,J.S., Narita,R., Morimoto,S., Takemura,A., Sambhara,S., Kawaguchi,A., Osari,S., Nagata,K., *et al.* (2012) Critical role of an antiviral stress granule containing RIG-I and PKR in viral detection and innate immunity. *PLoS One*, **7**, e43031.

47. Dennis,G., Sherman,B.T., Hosack,D.A., Yang,J., Gao,W., Lane,H.C. and Lempicki,R.A. (2003) DAVID: database for Annotation, Visualization, and Integrated Discovery. *Genome Biol.*, **4**, P3.
48. Thompson,J.D., Higgins,D.G. and Gibson,T.J. (1994) CLUSTAL W: improving the sensitivity of progressive multiple sequence alignment through sequence weighting, position-specific gap penalties and weight matrix choice. *Nucleic Acids Res.*, **22**, 4673–4680.
49. Timmer,J.C. and Salvesen,G.S. (2007) Caspase substrates. *Cell Death Differ.*, **14**, 66–72.
50. McStay,G.P., Salvesen,G.S. and Green,D.R. (2008) Overlapping cleavage motif selectivity of caspases: implications for analysis of apoptotic pathways. *Cell Death Differ.*, **15**, 322–331.
51. Julien,O. and Wells,J.A. (2017) Caspases and their substrates. *Cell Death Differ.*, **24**, 1380–1389.
52. Van Opdenbosch,N. and Lamkanfi,M. (2019) Caspases in cell death, inflammation, and disease. *Immunity*, **50**, 1352–1364.
53. Vigneswara,V. and Ahmed,Z. (2020) The role of caspase-2 in regulating cell fate. *Cells*, **9**, 1259.
54. Wu,Y., Zhao,D., Zhuang,J., Zhang,F. and Xu,C. (2016) Caspase-8 and Caspase-9 functioned differentially at different stages of the cyclic stretch-induced apoptosis in human periodontal ligament cells. *PLoS One*, **11**, e0168268.
55. He,B. (2006) Viruses, endoplasmic reticulum stress, and interferon responses. *Cell Death Differ.*, **13**, 393–403.
56. Banchereau,J. and Pascual,J. (2006) Type I interferon in systemic lupus erythematosus and other autoimmune diseases. *Immunity*, **25**, 383–392.
57. Takahashi,T., Nakano,Y., Onomoto,K., Yoneyama,M. and Ui-Tei,K. (2018) Virus sensor RIG-I represses RNA interference by interacting with TRBP through LGP2 in mammalian cells. *Genes (Basel)*, **9**, 511.
58. Satoh,T., Kato,H., Kumagai,Y., Yoneyama,M., Sato,S., Matsushita,K., Tsujimura,T., Fujita,T., Akira,S. and Takeuchi,O. (2010) LGP2 is a positive regulator of RIG-I- and MDA5-mediated antiviral responses. *Proc. Natl. Acad. Sci. U.S.A.*, **107**, 1512–1517.
59. Li,S., Yang,J., Zhu,Y., Wang,H., Ji,X., Luo,J., Shao,Q., Xu,Y., Liu,X. and Zheng,W. (2021) Analysis of porcine RIG-I like receptors revealed the positive regulation of RIG-I and MDA5 by LGP2. *Front. Immunol.*, **12**, 609543.
60. Parisien,J.P., Lenoir,J.J., Mandhana,R., Rodriguez,K.R., Qian,K., Bruns,A.M. and Horvath,C.M. (2018) RNA sensor LGP2 inhibits TRAF ubiquitin ligase to negatively regulate innate immune signaling. *EMBO J.*, **19**, e45176.
61. Quicke,K., Kim,K.Y., Horvath,C. and Suthar,M. (2019) RNA helicase LGP2 negatively regulates RIG-I signaling by preventing TRIM25-mediated caspase activation and recruitment domain ubiquitination. *J. Interferon Cytokine Res.*, **39**, 669–683.
62. Park,H., Davies,M.V., Langland,J.O., Chang,H.W., Nam,Y.S., Tartaglia,J., Paoletti,E., Jacobs,B.L., Kaufman,R.J. and Venkatesan,S. (1994) TAR RNA-binding protein is an inhibitor of the interferon-induced protein kinase PKR. *Proc. Natl. Acad. Sci. U.S.A.*, **91**, 4713–4717.
63. Takeuchi,K., Komatsu,T., Kitagawa,Y., Sada,K. and Gotoh,B. (2008) Sendai virus C protein plays a role in restricting PKR activation by limiting the generation of intracellular double-stranded RNA. *J. Virol.*, **82**, 10102–10110.
64. Zhang,S., Sun,Y., Chen,H., Dai,Y., Zhan,Y., Yu,S., Qiu,X., Tan,L., Song,C. and Ding,C. (2014) Activation of the PKR/eIF2α signaling cascade inhibits replication of Newcastle disease virus. *Virol. J.*, **11**, 62.
65. Matskevich,A.A. and Moelling,K. (2008) Stimuli-dependent cleavage of Dicer during apoptosis. *Biochem. J.*, **412**, 527–534.
66. Abou Zeid,L.Y., Shanmugapriya,S., Rumney,R.L. and Mosser,D.D. (2022) Caspase-mediated cleavage of miRNA processing proteins Drosha, DGCR8, Dicer, and TRBP2 in heat-shocked cells and its inhibition by HSP70 overexpression. *Cell Stress Chaperones*, **27**, 11–25.
67. Lee,J.Y., Moon,H.J., Lee,W.K., Chun,H.J., Han,C.W., Jeon,Y.W., Lim,Y., Kim,Y.H., Yao,T.P., Lee,K.H., *et al.* (2006) Merlin facilitates ubiquitination and degradation of transactivation-responsive RNA-binding protein. *Oncogene*, **25**, 1143–1152.
68. van der Veen,A.G., Maillard,P.V., Schmidt,J.M., Lee,S.A., Deddouche-Grass,S., Borg,A., Kjær,S., Snijders,A.P. and Reis e Sousa,C. (2018) The RIG-I-like receptor LGP2 inhibits Dicer-dependent processing of long double-stranded RNA and blocks RNA interference in mammalian cells. *EMBO J.*, **37**, e97479.
69. Komuro,A., Homma,Y., Negoro,T., Barber,G.N. and Horvath,C.M. (2016) The TAR-RNA binding protein is required for immunoresponses triggered by Cardiovirus infection. *Biochem. Biophys. Res. Commun.*, **480**, 187–193.
70. Miyamoto,M. and Komuro,A. (2017) PACT is required for MDA5-mediated immunoresponses triggered by Cardiovirus infection via interaction with LGP2. *Biochem. Biophys. Res. Commun.*, **494**, 227–233.
71. Lui,P.Y., Wong,L.R., Ho,T.H., Au,S.W.N., Chan,C.P., Kok,K.H. and Jin,D.Y. (2017) PACT facilitates RNA-induced activation of MDA5 by promoting MDA5 oligomerization. *J. Immunol.*, **199**, 1846–1855.
72. Sanchez David,R.Y., Combredet,C., Najburg,V., Millot,G.A., Beauclair,G., Schwikowski,B., Léger,T., Camadro,J.M., Jacob,Y., Bellalou,J., *et al.* (2019) LGP2 binds to PACT to regulate RIG-I- and MDA5-mediated antiviral responses. *Sci. Signal.*, **12**, eaar3993.

Received: June 29, 2023. **Revised:** March 14, 2024. **Editorial Decision:** March 16, 2024. **Accepted:** March 26, 2024